F^- formation via simultaneous two-electron capture during grazing scattering of F^+ ions from a LiF(001) surface

A. G. Borisov, V. Sidis, P. Roncin, A. Momeni, and H. Khemliche
Laboratoire des Collisions Atomiques et Moléculaires, UMR CNRS-Université Paris-Sud 8625, Université Paris-Sud, 91405 Orsay Cedex, France

A. Mertens and H. Winter
Institut für Physik, Humboldt-Universität zu Berlin, Invalidenstrasse 110, D-10115 Berlin, Germany
(Received 31 July 2002; revised manuscript received 11 October 2002; published 6 March 2003)

For slow F^+ ions ($v<0.05$ a.u.) scattered from a clean and flat LiF(001) surface under a grazing angle of incidence, large fractions of negative F^- ions have recently been observed in the reflected beam, while for neutral F^0 projectiles no negative F^- ions are produced in the same velocity range [P. Roncin *et al.*, Phys. Rev. Lett. **89**, 043201 (2002)]. From detailed studies on projectile energy loss and charge fractions, the conclusion was drawn that the F^- ions are formed from F^+ via a simultaneous capture of two electrons from adjacent F^- sites at the surface. We present a theoretical description of the double-electron-capture process leading to F^- formation from F^+ projectiles grazingly scattered from the LiF(001) surface. We use quantum chemistry calculations to determine the relevant Hamiltonian matrix and close-coupling solution of the time-dependent Schrödinger equation. The theoretical results are in good agreement with experimental observations.

DOI: 10.1103/PhysRevB.67.115403 PACS number(s): 79.20.Rf, 34.70.+e, 34.50.Dy

I. INTRODUCTION

In the past decade, considerable experimental and theoretical work has been devoted to studies on various phenomena in the scattering of atomic projectiles from the surfaces of alkali halides and oxides.[1–5] One motivation is the practical importance of ionic crystals for catalysis and optical applications. Another reason is the completely different electronic structure of ionic crystals in comparison to that of metals. Therefore, basic approaches and models developed for charge transfer between projectiles and metal surfaces[6] have to be substantially revised for ionic crystal targets.

The specific features of ionic insulators such as their point-charge lattices, wide band gaps, and narrow valence bands have been evoked to explain a variety of interesting observations such as, e.g., high electron yields,[5,7] discrete structures in the energy-loss spectra,[8–10] charge-transfer induced sputtering,[4,11–14] excitation of optical phonons,[15,16] formation of excited states at the surface,[9,10,17–19] and negative-ion formation in the scattered beams.[1–3,20–29] Of particular relevance for the understanding of the microscopic interaction mechanisms was the observation of large fractions of negative ions after the grazing scattering of fast projectiles from the surface of ionic crystals.[1,2,22–27] This finding is quite surprising at first in view of the large energy defect between the projectile affinity level (typically affinity is about 1–4 eV) and the valence-band states (binding energies$>$12 eV for LiF). The efficient negative-ion formation has been interpreted in terms of a sequence of binary collisions of projectiles with anions occupying halogen sites at the surface. *Only independent one-electron transitions have been considered*. For positive ions, this implies first, neutralization, and then the negative-ion conversion of the neutral projectile. For the latter process, the key feature is a drastic reduction of the energy defect of the charge-transfer reaction due to the attractive Coulomb interaction between the hole left at the surface and the negatively charged projectile in the final state of the charge transfer.[22–24] In the vicinity of halogen sites, the energy defect for electron capture is thus reduced to some eV giving rise to low-velocity thresholds for negative-ion formation. Furthermore, after a negative ion is formed, its direct detachment back to target states is blocked by the wide band gap of the ionic crystal, so that negative-ion populations get built up during the passage of projectiles from site to site. A model developed along these lines successfully reproduces the kinetic threshold behavior for the negative-ion conversion of neutral projectiles[22–24] (cf. Fig. 9).

The transfer of *several* electrons between a projectile and an ionic crystal surface has predominantly been studied for the neutralization of highly charged ions.[30–35] Traditional approaches developed for metal target surfaces are usually applied. So far, apart from the Auger process, multielectron transfer has been treated as a sequence of one-electron transitions in independent capture events. In this latter view, only the energy balance for a subsequent electron transfer depends on the state of the projectile prepared by the preceding electron transfer event. The apparent lack of theoretical approaches treating simultaneous transitions of several electrons is related to the missing experimental evidence for such processes. This is at variance with gas-phase collisions, where simultaneous multielectron transitions, such as two-electron transfer or excitation transfer, are well established and studied in detail with numerous examples involving highly charged ions.[36–38]

Recent experimental observations of the formation of F^- ions in the grazing scattering of F^+ projectiles from a LiF(001) surface showed evidence for the importance of simultaneous two-electron-capture events.[39] At low collision velocities, where no negative ions are formed with neutral F^0

projectiles, large fractions of negative ions in the scattered beam were observed for F^+ projectiles. In this case, the F^- ions cannot be produced in sequences of two independent steps: $F^+ \rightarrow F^0$, then $F^0 \rightarrow F^-$, because the second step is inefficient. From charge-transfer and energy-loss studies, it was concluded that the F^- formation from F^+ projectiles proceeds via the simultaneous capture of two electrons from adjacent F^- sites at the surface.

In this paper we present theoretical calculations of the F^- formation from F^+ projectiles and compare theoretical results with experimental data. We demonstrate that the ideas underlying the model of energy-level confluence—developed for the $F^0 \rightarrow F^-$ conversion[22–24]—can be also applied in the present case in order to explain the experimental results. The energy-level confluence occurs in the present case as a result of the Coulomb interaction between the negative projectile and the *two holes* left at the surface in the final state of the charge-transfer reaction. It is shown here that the $F^+ \rightarrow F^-$ conversion of the projectile with simultaneous capture of two electrons from adjacent F^- sites is a nearly resonant process. Since the F^+ ion has a $2p^4$ electronic shell structure, it may be produced in the ground $^3P^e$ and in the $^1D^e$ and $^1S^e$ excited metastable states. The implications of the presence of the latter states in the incident beam are discussed.

The paper is organized as follows. Section II is devoted to the presentation of the model. A qualitative discussion based on the point-charge approximation is also given in Sec. II and calculations are presented in Sec. III. Section IV is devoted to the discussion of the results, conclusions are drawn in Sec. V. In Appendixes A and B the details on quantum chemistry calculations are presented.

II. OUTLINE OF THE MODEL: POINT-CHARGE APPROXIMATION

A. General presentation of the model

The present theoretical treatment of F^- ion formation from F^+ projectiles is based on the general approach to charge-transfer processes at ionic crystal surfaces proposed in Ref. 24. This approach takes into account specific properties of ionic alkali halide crystals. Namely, the crystal lattice consists of $+1$ and -1 ions at the lattice cation (here Li^+) and anion (here F^-) sites. Valence-band (VB) electrons of the LiF crystal are formed by F^- $2p$ orbitals, which differ only slightly from the $2p$ orbitals of the free F^- ion.[40] The binding energy of the VB electrons is essentially the electron affinity of fluorine increased by the Madelung potential. The VB of LiF is narrow (width $\sim$3.5 eV) and it is separated from the conduction band by a 14-eV-wide band gap. LiF has a negative electron affinity with the bottom of the conduction band located at $\sim$2 eV above the vacuum level. Thus, 14 eV is needed to excite an electron from the valence to the conduction band, and $\sim$12 eV is needed to detach the VB electron from the surface. (For the electronic properties of the LiF crystal, see Refs. 41–44).

Owing to the localization of the VB electrons at F^- lattice sites, it has been demonstrated[24,45] that the one-electron transfer can be treated as a sequence of binary-type charge-transfer events, where an electron is transferred between the projectile and a given F^- site at the surface (active site). The finite VB width is neglected. It is assumed that removal of an electron from an F^- surface site leaves the corresponding hole localized at this site on the time scale of the binary collision event. Because of the narrow VB width of the LiF crystal, this approximation holds for the cases where the projectile is charged in the final state of the charge-transfer reaction.[45] The reason is that the interaction between the hole and the charge of the projectile lifts the degeneracy of the different F^- sites with respect to the hole localization. This transiently blocks the hole migration and keeps the hole at the active site during the charge-transfer event.

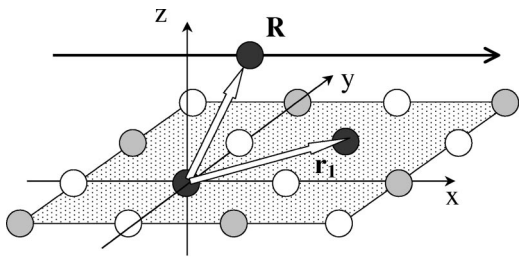

FIG. 1. Sketch of the considered system. The black circles are used for the projectile and the two ''active'' F^- sites at the LiF(001) surface constituting the active F_2^{2-} molecule. The **R** vector gives the position of the projectile. One of the active sites is located at the coordinate origin, while the other lies at an adjacent site at the surface with position given by the vector $\mathbf{r}_1$. The arrow parallel to the surface represents a segment of the grazing trajectory of the projectile.

Within the binary-type charge-transfer model for double-electron capture ($F^+ \rightarrow F^-$), we consider the interaction between the projectile and *two* active F^- sites at the surface. For energy reasons detailed below, the capture of two electrons from *the same* F^- site at the surface is inefficient. All other ions of the crystal lattice are considered as passive spectators and treated as point charges. Since the relaxation of the LiF surface is small,[46] we consider for the surface a simple termination of the bulk lattice structure with lattice constant $a = 7.68a_0$. The collision geometry considered in our calculations is sketched in Fig. 1. The projectile is located at **R**, and the two active F^- sites at the surface are located at the origin $\mathbf{r}_0 = (0,0,0)$ and $\mathbf{r}_1$. The two active F^- sites for the $F^+ \rightarrow F^-$ double-electron capture are adjacent. Other geometrical arrangements of active sites will not contribute to the two-electron charge-transfer process for energy reasons discussed below. We treat the negative-ion conversion of positive ions as a two-electron capture from the embedded F_2^{2-} ''active molecule'' formed by the two F^- ions at adjacent sites at the surface. The assumption that the $F^+ \rightarrow F^-$ conversion proceeds with two holes left at adjacent F^- sites at the surface is further supported by energy-loss measurements.[39] It is worth mentioning that the inclusion of the point charges is crucial for the correct description of the Madelung field of the crystal.

Concerning the effect of crystal polarization, *at the instant of charge transfer* the local charge of the complex formed by the projectile and active site(s) is left unchanged as seen from the rest of the crystal. Then, the screening effects by the

rest of the crystal are not expected to bring sizable corrections to the energy difference between initial and final states.[12,45,47,48] When the projectile escapes from the charge-transfer region, the crystal polarization given by Mott-Littleton terms[49,50] produces additional screening providing correct *asymptotic* energy differences.

B. Simple estimates for the energetics of electron transfer

The efficiency of any charge-transfer reaction strongly depends on the energy difference between initial and final states at the instant of the transition. For charge transfer at a LiF(001) surface, this energy difference can be estimated from the point-charge model which yields results in reasonable agreement with quantum chemistry studies. Since the $F^+ \rightarrow F^-$ conversion can be considered either as a one-step process or a two-independent-step process, we are interested in the energetics of the following three charge-transfer reactions: $F^+ \rightarrow F^0$ (neutralization), $F^0 \rightarrow F^-$ (negative-ion conversion of a neutral projectile), and $F^+ \rightarrow F^-$ (direct negative-ion conversion of a positive projectile).

1. Positive-ion neutralization

For the neutralization of a positive ion ($F^+ \rightarrow F^0$), we consider electron capture from the active F^- site located at the coordinate origin. The energy defect for the neutralization is given by the difference between the energy E_{II} of the final state (F^0 projectile $+ F^0$ at active site located at the origin) and the energy E_{I} of the initial state (F^+ projectile $+ F^-$ at active site): $\Delta E(\mathbf{R}) = E_{\mathrm{II}}(\mathbf{R}) - E_{\mathrm{I}}(\mathbf{R})$. As detailed in Ref. 24, within the point-charge model, $\Delta E(\mathbf{R})$ is given by

$$\Delta E(\mathbf{R}) = -I + \left(A + \sum_{i \neq 0} \frac{q_i}{|\mathbf{r}_i|} \right) - \sum_i \frac{q_i}{|\mathbf{r}_i - \mathbf{R}|}, \qquad (1)$$

where q_i is the charge of an ion of the crystal lattice located at $\mathbf{r}_i$. Note that owing to the open-shell structure of the F^+ ion ($1s^2 2s^2 2p^4$), the incident F^+ beam consists, for our experimental conditions, of $F^+(^3P)$ ground-state ions and long-lived excited species $F^+(^1D)$ and $F^+(^1S)$. I is the ionization potential of the F^0 atom with respect to the ground or excited states of the F^+ ion involved in the electron transfer. It amounts to 17.42 eV with respect to the ground ^3P state, 20.01 eV with respect to the ^1D state, and 22.99 eV with respect to the ^1S state. A is the electron affinity of the fluorine atom (3.4 eV). In the point-charge approximation, a crystal with a neutralized F^- site at the surface is equivalent to a perfect crystal plus one additional positive charge localized at this site. The first sum in Eq. (1) gives the interaction energy between this positive charge located at the origin and the rest of the crystal. This is the Madelung potential of LiF for a surface site (12.05 eV). Thus, the term in parentheses gives the classical estimate for the electron binding energy at a F^- surface site (15.45 eV). The last term in Eq. (1) results from the electrostatic interaction between the positive projectile and a perfect LiF crystal in the initial state of the charge-transfer reaction. Due to the neutrality of the LiF crystal, it is small and amounts to about 1 eV only. Thus, the energy defect for the neutralization of positive ions is almost constant and is given by the difference in binding energies of electrons in the valence band of the LiF crystal and in the free F^0 atom.

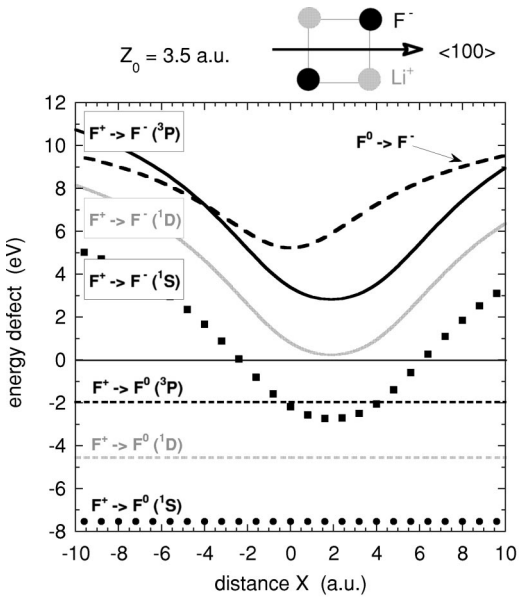

FIG. 2. The energy differences ΔE for the different charge-transfer reactions calculated within the point-charge model [Eqs. (1)–(3)]. The data are represented as functions of the distance X along the straight-line trajectory in the $\langle 100 \rangle$ direction as schematically shown in the inset: $\mathbf{R} = (X, Y_0 = a/4, Z_0 = 3.5 \text{ a.u.})$. $a = 7.59 a_0$ is the LiF lattice constant. The reference frame is oriented as shown in Fig. 1. The thin solid line gives the position of the energy reference.

2. Negative-ion conversion of a neutral projectile

Following the point-charge model and discussion in Ref. 24 for the negative-ion conversion of the neutral projectile ($F^0 \rightarrow F^-$), the energy difference between the initial state (F^0 projectile $+ F^-$ at the active site located at the coordinate origin) and the final state (F^- projectile $+ F^0$ at the active site) is given by

$$\Delta E(\mathbf{R}) = -A + \left(A + \sum_{i \neq 0} \frac{q_i}{|\mathbf{r}_i|} \right) + \sum_i \frac{(-1) q_i}{|\mathbf{r}_i - \mathbf{R}|} - \frac{1}{|\mathbf{R}|}. \qquad (2)$$

The last term in Eq. (2) is the basis for the efficient negative-ion conversion of neutral projectiles by the energy-level confluence between initial and final states. This is the Coulomb interaction between the hole left at the surface and a negative projectile in the final state of the charge-transfer reaction, which reduces ΔE from the asymptotic 12 eV range down to 5 eV in the charge-transfer region (see Fig. 2).

3. Negative-ion conversion of a positive ion

Finally, we consider the energy difference between the initial and final states for negative-ion conversion of a positive ion ($F^+ \rightarrow F^-$), where two active F^- sites at the surface provide two electrons. The energy E_{I} of the initial state (F^+ projectile and two F^- ions at the active sites located at $\mathbf{r}_0$ and $\mathbf{r}_1$) is given by

$$E_{\mathrm{I}}(\mathbf{R}) = E(\mathrm{F}^+) + E(\mathrm{F}^-) + E(\mathrm{F}^-) + \frac{1}{2}\sum_{i\neq j}\frac{q_i q_j}{r_{ij}} + \sum_i \frac{(+1)q_i}{|\mathbf{r}_i - \mathbf{R}|}, \tag{3a}$$

where $E(\mathrm{F}^{+(-)})$ is the total energy of the free $\mathrm{F}^{+(-)}$ ion. The first sum gives the interaction energy between the point charges of the LiF lattice with $r_{ij}=|\mathbf{r}_i-\mathbf{r}_j|$, the last term describes the interaction of the positive projectile with a perfect LiF crystal. The energy of the final state (F^- projectile and two F^0 ions at the active sites) is given by

$$E_{\mathrm{II}}(\mathbf{R}) = E(\mathrm{F}^-) + E(\mathrm{F}^0) + E(\mathrm{F}^0) + \frac{1}{2}\sum_{i\neq j}\frac{q_i q_j}{r_{ij}} + \sum_{i\neq 0}\frac{(+1)q_i}{r_{0,i}} + \sum_{i\neq 1}\frac{(+1)q_i}{r_{1i}} + \frac{1}{|\mathbf{r}_0-\mathbf{r}_1|} + \sum_i \frac{(-1)q_i}{|\mathbf{r}_i-\mathbf{R}|} + \frac{(-1)}{|\mathbf{r}_0-\mathbf{R}|} + \frac{(-1)}{|\mathbf{r}_1-\mathbf{R}|}. \tag{3b}$$

Here we use the fact that the field of the crystal with two neutralized sites can be represented as the field of a perfect crystal plus two additional positive charges localized at positions $\mathbf{r}_0$ and $\mathbf{r}_1$. The energy defect for the two-electron capture is given by

$$\Delta E(\mathbf{r}) = -(I+A) + \left\{A + \sum_{i\neq 0}\frac{q_i}{r_{0i}}\right\} + \left\{A + \sum_{i\neq 1}\frac{q_i}{r_{1i}}\right\} - 2\sum_i \frac{q_i}{|\mathbf{r}_i-\mathbf{R}|} + \frac{1}{|\mathbf{r}_0-\mathbf{r}_1|} - \left[\frac{1}{|\mathbf{r}_0-\mathbf{R}|} + \frac{1}{|\mathbf{r}_1-\mathbf{R}|}\right]. \tag{3c}$$

The meaning of the terms in Eq. (3c) is straightforward. The first three terms represent the binding-energy difference between the two valence-band electrons in LiF and the two electrons in the F^- projectile. The fourth term originates from the point-charge interactions with a perfect LiF surface and is small. The fifth term corrects the binding energy of two valence-band electrons in the LiF crystal for the (unscreened) hole-hole interaction in the final state. For two holes located at adjacent F^- sites of the surface, we have $r_{01}=a/\sqrt{2}$. This gives for the unscreened hole-hole interaction energy a value of 5 eV. The **R** dependence of the energy defect for the two-electron transfer reaction is mainly given by the last term in square brackets in Eq. (3c). Similarly to the one-electron transfer for the $\mathrm{F}^0\rightarrow\mathrm{F}^-$ case [Eq. (2)] this term describes the attractive Coulomb interaction between the two holes left at the surface and a negative projectile in the final state of the charge-transfer reaction. Owing to this term, the energy defect of the charge transfer can be brought down to the sub-eV range (see Figs. 2 and 5).

Finally, we consider the F^- conversion of the F^+ projectile with the two electrons captured from *the same* F^- site at the surface. Using the above approach, we get

$$\Delta E(\mathbf{R}) = 2\sum_{i\neq 0}\frac{q_i}{|\mathbf{r}_i|} - 2\sum_i \frac{q_i}{|\mathbf{r}_i-\mathbf{R}|} - \frac{2}{|\mathbf{R}|}. \tag{4}$$

This is at least twice the energy defect for F^- ion formation from F^0 projectiles [compare with Eq. (2)]. The large value of the energy defect makes the direct capture of the two electrons from the same F^- site at the surface very unlikely at low projectile energies. This is confirmed by our experiments.

C. Qualitative discussion

The energy defects given by Eqs. (1), (2), and (3c) are shown in Fig. 2 as functions of the X coordinate for a projectile trajectory parallel to the surface in the $\langle 100\rangle$ direction $\mathbf{R}=(X,Y_0,Z_0)$ with $Z_0=3.5a_0$ a typical distance of the turning point for low-energy grazing scattering experiments, and $Y_0=a/4$. For this trajectory, the oscillating field created by the alternating rows of positive and negative charges is 0, so that the figure displays the major trends of the energy defects $\Delta E(\mathbf{R})$.

As seen in Fig. 2, neutralization of F^+ projectiles in a binary-type charge transfer is an exothermic reaction with an energy defect of about -2 eV for the ground-state ions and -4 eV and -8 eV for the excited metastable species. For F^- ion formation in the $\mathrm{F}^0\rightarrow\mathrm{F}^-$ charge transfer, the energy defect is about 5 eV. As for the direct $\mathrm{F}^+\rightarrow\mathrm{F}^-$ charge-transfer reaction via double-electron capture from neighboring F^- sites, it is seen to proceed with a much lower energy defect. Thus, on the basis of the point-charge model, one can draw some conclusions on the efficiency of the different charge-transfer reactions occurring in F^+ grazing scattering from the LiF(001) surface. Both, $\mathrm{F}^+\rightarrow\mathrm{F}^0$ and $\mathrm{F}^0\rightarrow\mathrm{F}^-$ single-electron-capture processes correspond to charge-transfer reactions with finite energy defects above 2 eV, so that the electron transfer probability should exhibit a threshold behavior as a function of projectile velocity. The double-electron-capture process $\mathrm{F}^+\rightarrow\mathrm{F}^-$ with two electrons captured from adjacent F^- sites at the LiF(001) might be a quasiresonant process, depending on the state of the F^+ ion. This should lead to very low velocity thresholds (if any) and high efficiency of the direct $\mathrm{F}^+\rightarrow\mathrm{F}^-$ conversion at low energies.

III. CALCULATIONS OF THE DYNAMICS OF THE CHARGE-TRANSFER PROCESS

A. Description of the binary charge transfer

As explained above, we consider the charge-transfer process in grazing scattering of F^+ projectiles from a LiF surface as a succession of binary-type electron transfer events between the F^+ projectile and an active molecule $\mathrm{F}_2{}^{2-}$ formed by two F^- ions at adjacent sites of the LiF(001) surface. All other ions of the LiF(001) surface are included as point charges. This approach is thus close to the *active cluster* studies.[20,45,51,52] The motion of the projectile is treated classically and the electronic subsystem is described quantum mechanically. Since the total electronic spin is conserved in the transitions, the triplet and singlet symmetries

are treated independently. The time-dependent electronic wave function is expanded over a (quasi-) diabatic basis representing the states of the charge-transfer arrangements $F^+ + {F_2}^{2-}$, $F^0 + {F_2}^-$, and $F^- + {F_2}^0$ of the projectile plus active molecule system:

$$\Psi(\{\boldsymbol{\rho}\},\mathbf{R},t) = \sum_j A_j(t)\Phi_j(\{\boldsymbol{\rho}\};\mathbf{R}), \tag{5}$$

where $\{\boldsymbol{\rho}\}$ denotes electronic coordinates. In this equation the dependence of the basis functions on the projectile coordinates is weak. It arises from the orthogonalization of atomic orbitals of the projectile to molecular orbitals of the active molecule. For more details on the definition of the basis see Appendix A.

The functions $\Phi_j(\{\boldsymbol{\rho}\};\mathbf{R})$ are arranged in groups, each of which represents a charge-transfer arrangement of the collisional system. For the *singlet* symmetry, we have $1 \leqslant j \leqslant 33$. The six lowest states describe the incident channel, with $j=1$ corresponding to the $F^+(^1S)$ ion in front of the ${F_2}^{2-}$ molecule, and $j=2,...,6$ corresponding to five magnetic substates of the $F^+(^1D)$ ion in front of the ${F_2}^{2-}$ molecule (incident channels). The $\Phi_j(\{\boldsymbol{\rho}\};\mathbf{R})$ functions with higher j describe the electron transfer from the surface to the projectile. Thus, 18 states with $j=7,...,24$ correspond to the neutralization of the F^+ ion and describe the neutral F^0 projectile bearing a hole in the $2p_x$, $2p_y$, or $2p_z$ orbital in front of the ${F_2}^-$ molecule with a hole in one of the six molecular orbitals formed by the mixture of the $2p$ orbitals of the F^- ions at the surface. The nine states with $j=25,...,33$ correspond to the negative-ion conversion of the F^+ ion and describe the F^- projectile in front of the F_2 molecule with two holes in the valence shell. The latter nine F_2 states are unambiguously identified as those that are formed by two F^0 atoms. Other F_2 states are formed by configurations with two holes located at the same F^- ion of the active molecule. These states have much higher energies and are therefore not included in the calculation. For the triplet symmetry we have $1 \leqslant j \leqslant 30$, where the first three states correspond to the incident channel with a $F^+(^3P)$ ion in front of the ${F_2}^{2-}$ molecule. The next 18 and then nine states correspond to the $F^0 + {F_2}^-$ and $F^- + {F_2}^0$ arrangements, respectively. It is worth mentioning that, in order to keep the calculation size reasonable, we have not included in the treatment the basis functions corresponding to the electron transfer to surface exciton and trion states[9,10,17,18] as well as to the conduction band.[51,52] Therefore, the processes of charge transfer resulting in the formation of excited states at the surface are inaccessible for the present treatment. In any case, at low projectile velocities these processes are thought to be due to the intermediate negative-ion formation.[9,10,17–19]

Inserting Eq. (5) into the time-dependent Schrödinger equation leads to the set of coupled equations for the amplitudes:

$$i\frac{dA_j(t)}{dt} + i\sum_k A_k(t)\langle\Phi_j|\mathbf{v}\cdot\boldsymbol{\nabla}_{\mathbf{R}}\Phi_k\rangle = \sum_k A_k(t)\langle\Phi_j|H|\Phi_k\rangle, \tag{6}$$

where $\mathbf{v}$ is the velocity of the projectile and the integration in Eq. (6) concerns the electronic coordinates. For the considered basis and low projectile velocities, the gradient couplings at the left-hand side of Eq. (6) can be neglected, so that finally we obtain the set of coupled equations for the amplitudes A_j:

$$i\frac{dA_j(t)}{dt} = \sum_k H_{jk}A_k(t). \tag{7}$$

We use the quantum chemistry code[53] GAMESS to calculate the matrix elements H_{jk} in the basis of states Φ_j. The details are given in Appendix A. Given the Hamiltonian matrix, the amplitudes A_j are calculated from Eq. (7) via the Lanczos time-propagation technique.[54] The set of initial conditions $A_j(t=0)=\delta_{jk}$ corresponds to the different substates of the incident F^+ ion.

B. Population build up

For grazing scattering the trajectories of the projectile are well represented by a piecewise approximation with long paths traveled parallel to the surface at a fixed distance. Therefore, we first solve Eq. (7) for projectile trajectories lying in the plane parallel to the surface at a distance Z, and spanning a two-dimensional (2D) surface cell containing the ${F_2}^{2-}$ molecule $\mathbf{R}(t)=(\mathbf{r}_{2D}+\mathbf{v}_{\|}t,Z)$ (Figs. 1 and 3). $\mathbf{v}_{\|}$ is the projectile velocity component parallel to the surface and $\mathbf{r}_{2D}$ is the impact parameter. Since the calculations for random orientations of the projectile trajectory are very time consuming, we study the charge transfer for projectile scattering close to the $\langle 100\rangle$ and $\langle 110\rangle$ directions. The charge fractions obtained in both cases are found to be very similar. This supports, *a posteriori*, the validity of the comparison between the present theoretical results and the experimental data[39] taken at random azimuthal directions. As schematically shown in Fig. 3, for the projectile scattering close to the $\langle 100\rangle$ direction (x axis), we consider projectile trajectories $\mathbf{R}(t)=(v_{\|}t,Y,Z)$ with impact parameters $0 \leqslant Y \leqslant L=a/2$. For projectile trajectories close to the $\langle 110\rangle$ direction, two orientations of the active ${F_2}^{2-}$ molecules contribute to the charge transfer. For both orientations, taking into account symmetry, we use projectile trajectories given by $\mathbf{R}(t) = (v_{\|}t/\sqrt{2}, Y+v_{\|}t/\sqrt{2}, Z)$ with $0 \leqslant Y \leqslant L=a/2$.

For a given impact parameter Y and initial condition $A_j(t=0)=\delta_{jk}$, related to an incident F^+ ion state (^1S, ^1D, or ^3P), the probabilities of neutralization, P^0, and negative-ion formation, P^-, are given by

$$P^{0(-)}_{^1S}(Y,Z,k) = \sum_{j=7(25)}^{24(33)} |A_j(t\to\infty)|^2, \quad k=1,$$

$$P^{0(-)}_{^1D}(Y,Z,k) = \sum_{j=7(25)}^{24(33)} |A_j(t\to\infty)|^2, \quad k=2,...,6, \tag{8}$$

$$P^{0(-)}_{^3P}(Y,Z,k) = \sum_{j=4(22)}^{21(30)} |A_j(t\to\infty)|^2, \quad k=1,2,3.$$

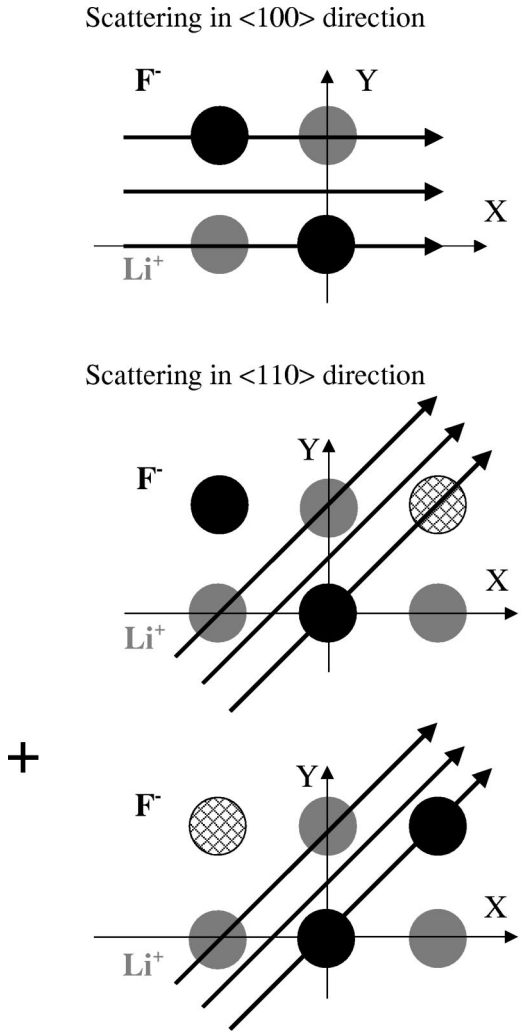

FIG. 3. Sketch of the directions of the projectile trajectories used to obtain the average neutralization and negative-ion formation probabilities per active F_2^{2-} molecule. Black circles, active F^- lattice sites; gray circles, Li^+ ions considered as point charges; shaded circles, F^- ions considered as a point charges. Note that two possible orientations of the projectile trajectories with respect to the active F_2^{2-} molecule have to be taken into account for scattering in the $\langle 110 \rangle$ direction.

From the neutralization and negative-ion formation probabilities given by Eq. (8) we obtain the average probabilities for the neutralization and negative-ion formation in binary collision with a F_2^{2-} molecule. For example, for the $F^+(^3P)$ incident state of the positive ion, we have

$$P_{^3P}^{0(-)}(Z)=\frac{1}{3}\sum_{k=1}^{3}\frac{2}{L}\int_0^{L/2}P_{^3P}^{0(-)}(Y,Z,k)dY. \tag{9}$$

The projectile beam scattered from the surface in a given direction will cross the successive 2D cells containing the active F_2^{2-} molecules at instants t_m and at distances Z_m. The evolution of charge states along the trajectory can be expressed, e.g., for the ^3P channel, as

$$\begin{aligned} n_m^-(^3P)&=n_{m-1}^-(^3P)+n_{m-1}^+(^3P)P_{^3P}^-(Z_m)\\ &\quad+n_{m-1}^0(^3P)\Pi^-(Z_m),\\ n_m^0(^3P)&=n_{m-1}^0(^3P)[1-\Pi^-(Z_m)]+n_{m-1}^+(^3P)P_{^3P}^0(Z_m),\\ n_m^+(^3P)&=1-\{n_m^0(^3P)+n_m^-(^3P)\}, \end{aligned} \tag{10}$$

where n stands for the population of different charge states. Equation (10) incorporates the possibility of negative-ion formation from the neutral projectile by one-electron capture from the F^- sites at the surface. The probabilities of this process $\Pi^-(Z_k)$ have been calculated in Ref. 24. These probabilities show a threshold behavior with projectile velocity ($v_{\rm th}\sim 0.06$ a.u., see Fig. 9). Finally, the resulting charge fractions in the scattered beam $N^{+,0,-}$ are obtained from the statistical average over the different states of the incident F^+ ions. Provided that all substates of the F^+ ion are present in the incident beam, one obtains

$$N^{+,0,-}=[n_{m\to\infty}^{+,0,-}(^1S)+5n_{m\to\infty}^{+,0,-}(^1D)+9n_{m\to\infty}^{+,0,-}(^3P)]/15. \tag{11}$$

C. Calculation of the trajectory

In the case of grazing scattering (surface channeling conditions[55]) the trajectory of the projectile is determined by the effective potential $U(Z)$, a function of projectile-surface distance only. The effective scattering potential for F^+ projectiles is given by

$$\begin{aligned} U(Z)&=\left\langle \sum_{F^-} V_{F^-/F^+}(\mathbf{R}-\mathbf{r}_{F^-})+\sum_{Li^+} V_{Li/F^+}(\mathbf{R}-\mathbf{r}_{Li^+})\right\rangle_{X,Y}\\ &\quad+U_{\rm im}(Z), \end{aligned} \tag{12}$$

where V_{F^-/F^+} and V_{Li^+/F^+} are binary interaction potentials between projectile and halide and alkali-metal sites, respectively. These binary interaction potentials are determined from Hartree-Fock-Roothaan self-consistent-field (SCF) calculations (see Ref. 24). In Eq. (12), the summations run over the halogen (alkali-metal) surface sites; the averaging is performed over all possible positions of the projectile in the (x,y) plane parallel to the surface. $U_{\rm im}(Z)$ is the image potential created by the response of the crystal to the presence of the moving charge.

The image potential is calculated on the basis of the surface response formalism.[56,57] For a particle with charge Q and velocity v moving parallel to the surface, the image potential is given by

$$U_{\rm im}(Z)=-\frac{Q}{\pi v}\int_0^\infty d\omega\, K_0\left(\frac{2\omega Z}{v}\right){\rm Re}\left(\frac{\varepsilon(\omega)-1}{\varepsilon(\omega)+1}\right), \tag{13}$$

where K_0 is the modified Bessel function of order 0. We use the surface response function $[\varepsilon(\omega)-1]/[\varepsilon(\omega)+1]$ with the dielectric constant $\varepsilon(\omega)$ deduced from optical data for LiF.[58] The resulting image potentials are shown in Fig. 4 as

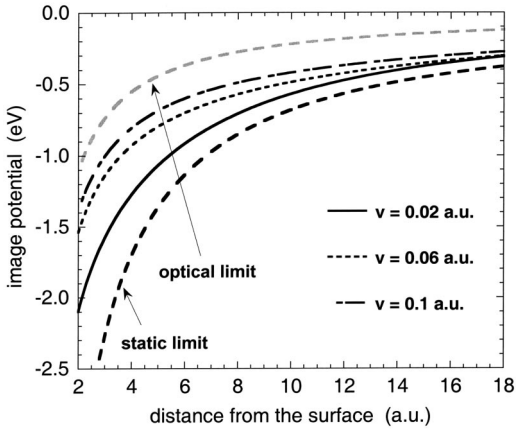

FIG. 4. Image potentials obtained from Eq. (13) for different collision velocities. The results are presented as functions of the distance from the surface. Black and gray long dashed lines give, respectively, the static and optical limits as indicated in the figure.

functions of the projectile surface distance Z and for different projectile velocities. Depending on the collision velocities, both electrons and ions or only electrons of the crystal respond to the field of the projectile. Correspondingly, $U_{\rm im}(Z)$ spans values between the static limit and the optical limit with dielectric constants $\varepsilon_0=9.01$ and $\varepsilon_\infty=1.96$.[58,59]

IV. RESULTS AND DISCUSSION

A. Structure of the Hamiltonian matrix and theoretical binary charge-transfer probabilities

Figure 5 shows the diabatic energies of the different states given by the diagonal elements H_{jj} of the Hamiltonian matrix as obtained from our quantum chemistry calculations described in Appendix A. They are compared with the point-charge model prediction. Energies refer to the middle of the band formed by $F_2^- + F^0$ states at infinite separation between the projectile and the surface. The energies of these states denoted by black circles describe final states for *one-electron transfer* with neutralization of the positive projectile. At infinite projectile distance from the surface, the manifold of nondegenerate states corresponds to the hole localization at different orbitals of the F_2^{2-} molecule, it reflects the beginning of the formation of the valence band of the LiF crystal. Diamonds and crosses represent energies of the states corresponding to the incident channel (F^+ projectile$+F_2^{2-}$ molecule). For singlet symmetry, crosses represent the state of the $F^+(^1S)$ ion, and diamonds represent five nearly degenerate states of the $F^+(^1D)$ ion. For triplet symmetry, diamonds represent three nearly degenerate states of the $F^+(^3P)$ ion. The band of states given by open circles corresponds to states bearing two holes in the F_2^{2-} molecular orbitals. These states thus describe the (F^- projectile$+F_2$ molecule) arrangement and correspond to the negative-ion conversion of positive projectiles.

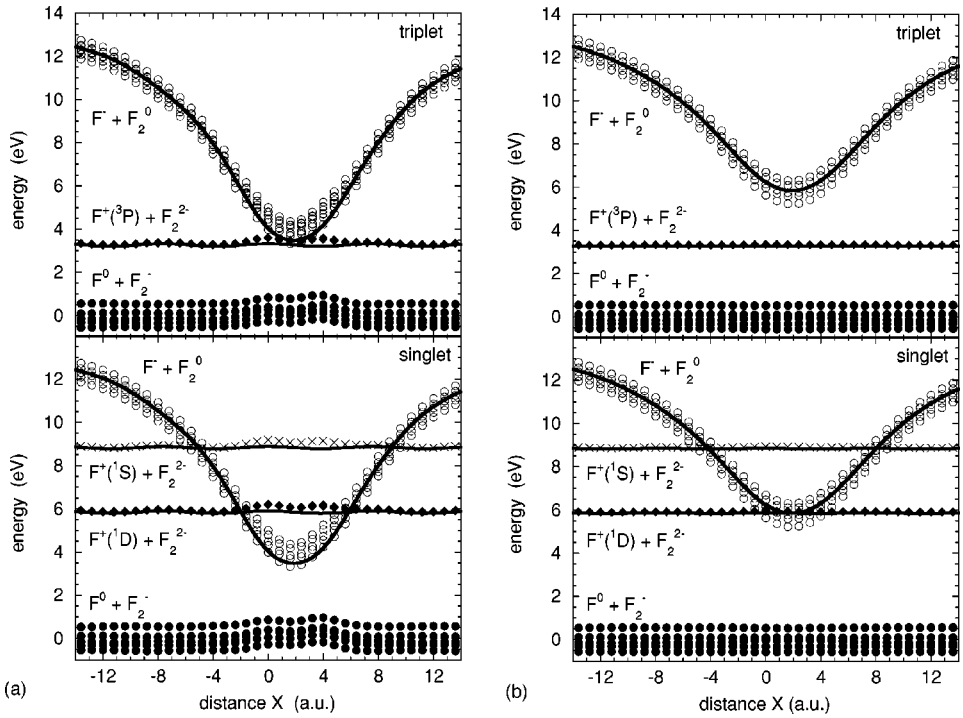

FIG. 5. (a) The relative energies of the different diabatic states involved in the F^+ charge exchange with the active F_2^{2-} molecule. The two panels correspond to the triplet (upper panels) and singlet (lower panel) total electronic spin of the system. The data are represented as functions of the distance X along a straight-line trajectory in the $\langle 100\rangle$ direction: $\mathbf{R}=(X,Y_0=a/4,Z_0=3.5$ a.u.). The energy reference is taken as the middle of the manifold of states corresponding to the one-electron transfer from the surface to the projectile, i.e., to the $F^0+F_2^-$ arrangement. Symbols, quantum chemistry results; solid lines, results of the point-charge model corrected for the $I_{\rm LiF}=14.11$ eV position of the middle of the valence band (see Appendix B). The manifolds of the states are labeled according to the gross charge-transfer arrangements. For more details see the text. (b) Same as (a) but for $\mathbf{R}=(X,Y_0=a/4,Z_0=4.75$ a.u.).

As a first observation, the point-charge model, when corrected to the self-consistent-field results for the electron binding energy in the LiF crystal, $I_{\mathrm{LiF}}=14.11$ eV (see Appendix B), reproduces the quantum chemistry calculations. This supports the simple interpretation given in Sec. II for the efficiency of the different charge-transfer reactions.

For the impact parameter Y chosen here, the energy defect for the *neutralization* of positive ions is essentially independent of the X coordinate of the projectile and its distance from the surface. This energy defect is larger for the excited states of the F^+ ion, which should lead to higher collision velocity thresholds for the neutralization. The energy-level confluence is observed for the two-electron capture with negative-ion conversion of the positive projectiles. For projectile trajectories along the $\langle 100\rangle$ direction at the distance $Z=3.5a_0$ from the surface, *negative-ion conversion* of the ground-state $F^+(^3P)$ projectiles is a quasiresonant process. As for the metastable $F^+(^1S)$ and $F^+(^1D)$ channels, a diabatic energy curve crossing is observed. At small separations between the projectile and the $F_2{}^{2-}$ active molecule, where the charge-transfer couplings are efficient, the F^- conversion of the $F^+(^1D)$ ions proceeds with an energy defect of ~ 2 eV. As for the $F^+(^1S)$ projectiles, the energy defect is too large, so that the negative-ion conversion should be inefficient at small projectile velocities as supported by our charge-transfer studies.

When the distance between the projectile and the surface is increased [see Fig. 5(b)], the energy-level confluence is less pronounced. Then during the scattering event, the projectile will pass distances from the surface, here $Z_0 \sim 4.75a_0$, where the negative-ion formation from $F^+(^1D)$ ions is a resonant process as shown in Fig. 5(b). Note that in this case the negative-ion conversion of the $F^+(^3P)$ proceeds with a finite-energy defect. *A priori*, for even larger distances Z, the $F^+(^1S)$ channel is moved to resonance with respect to the double-electron-capture process. However, as supported by our studies, the charge-transfer couplings get too small for the negative-ion conversion of the $F^+(^1S)$ ions to take place.

The velocity-dependent binary charge-transfer probabilities are presented in Fig. 6 for $F^+(^3P)$ and $F^+(^1D)$ ions incident at the surface close to the $\langle 100\rangle$ direction, and $Z_0=3.5a_0$ and $Z_0=4.75a_0$. As for the $F^+(^1S)$ incident channel, we find that the scattering process is elastic and charge transfer does not take place. From this finding we conclude that the fraction of the survived F^+ ions in the experiment should be at least of the order of $\frac{1}{15}$, i.e., the statistical weight of the ^1S channel.

The results shown in Fig. 6 can be understood from the energies of the different states depicted in Fig. 5. For $Z_0=3.5a_0$ and incident F^+ ions in the ^1D and ^3P state, double-electron capture with F^- formation occurs at projectile velocities as low as 0.02 a.u. The fraction of negative ions in one binary collision event is of the order of 1% with incident $F^+(^1D)$ ions and reaches 40–50 % with incident $F^+(^3P)$ ions. This result reflects an almost perfect energy matching for the F^-+F_2 and $F^+(^3P)+F_2{}^{2-}$ states and a finite-energy defect for the $F^+(^1D)$ channel. While the negative ions are efficiently formed at low projectile velocities, the neutralization of F^+ via one-electron capture is blocked because of the relatively large energy defect of the charge-transfer reaction. The velocity onset for neutralization is lower for $F^+(^3P)$ projectiles than for $F^+(^1D)$ projectiles because of the smaller energy defect for charge transfer. Note that for the double-electron capture, the neutralization of positive ions is a competing channel. This is manifested by a decrease of the negative-ion formation probability for increasing neutralization probability. With $Z_0=4.75a_0$ [Fig. 6(b)] the overall charge-transfer probabilities are smaller because of decreased couplings. The negative-ion conversion of $F^+(^3P)$ projectiles gets suppressed because of the finite-energy defect of the charge-transfer reaction. As for the resonant $F^+(^1D)$ channel, the negative-ion conversion is of the order of 1% and exhibits the same velocity dependence as observed for the $F^+(^3P)$ channel with $Z_0=3.5a_0$ [Fig. 6(a)].

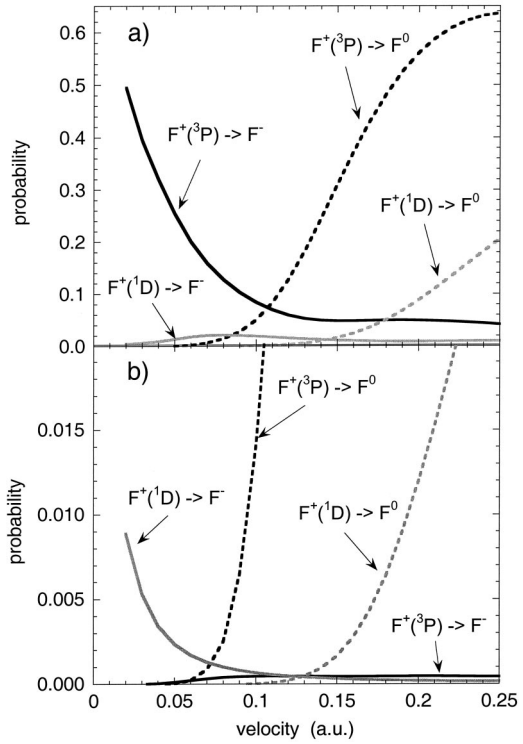

FIG. 6. (a) Probabilities $P^{0(-)}_{^3P(^1D)}(Z_0)$, averaged over the impact parameters Y [see Eq. (9)] for negative-ion formation (solid lines) and neutralization (dashed lines) in a binary collision with the active $F_2{}^{2-}$ molecule. Distance from the surface $Z_0=3.5a_0$. The projectile trajectories are oriented in the $\langle 100\rangle$ direction. Black and gray colors correspond to the different initial states of the incident F^+ ion: $F^+(^3P)$ and $F^+(^1D)$, respectively. The data are presented as functions of the projectile velocity. (b) Same as (a) but for $Z_0=4.75a_0$.

To analyze the driving force of the two-electron-capture processes leading to direct negative-ion conversion of positive ions, we have performed time-dependent studies of the charge transfer with a modified Hamiltonian matrix $\tilde{H}$. $\tilde{H}$ differs from H in that all one-electron couplings (A_{1e},B_{1e}) between the corresponding groups of states, $F^++F_2{}^{2-}$ and $F^0+F_2{}^-$, $F^0+F_2{}^-$, and F^-+F_2, have been set to zero (see Fig. 7). We maintain only the dielectronic couplings (W_{2e}) between the $F^++F_2{}^{2-}$ and F^-+F_2 states. The binary

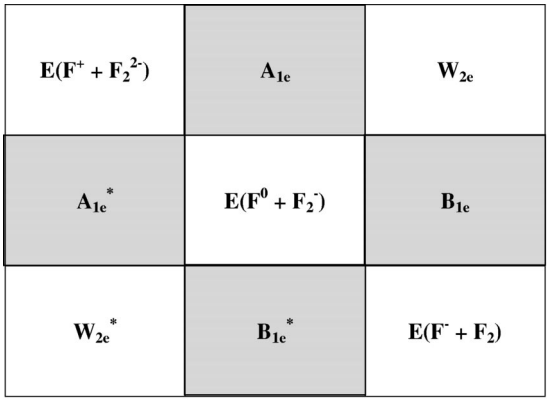

FIG. 7. Schematic, 3×3, representation of the Hamiltonian matrix of the charge-transfer system. W_{2e} stands for the direct two-electron coupling terms between the $F^+ + F_2{}^{2-}$ and $F^- + F_2$ configurations. A_{1e} and B_{1e} denote the one-electron coupling terms between the $F^+ + F_2{}^{2-}$ and $F + F_2{}^-$ and $F + F_2{}^-$ and $F^- + F_2$ configurations, respectively.

charge-transfer probabilities for negative-ion formation obtained in that case are at least two orders of magnitude smaller than those shown in Fig. 6. This result shows that the negative-ion conversion of the positive projectile is a second-order process induced by one-electron couplings. As a general trend, similar conclusions on the nature of the interactions responsible for the simultaneous double-electron transfer in gas-phase collisions have been derived.[38]

B. Charge fractions of scattered beams

In Fig. 8 we show results for charge fractions of the outgoing beam resolved with respect to the state of the incident F^+ ions. In both cases, negative ions are efficiently formed well below the neutralization threshold and the threshold for negative-ion formation from neutral atoms. If negative-ion formation from F^0 projectiles is not included in the calculations, negative-ion fractions decrease at higher velocities. This feature was already discussed for the binary charge-transfer probabilities plotted in Fig. 6. The reason for the decrease of negative-ion formation at velocities above the F^+ neutralization threshold is that the competing channel (one-electron capture from $F_2{}^{2-}$ molecules with F^0 formation) takes most of the flux. Indeed, since the single-electron capture ($F^+ \rightarrow F^0$) is a first-order process with respect to one-electron couplings, it is more probable than the double-electron capture ($F^0 \rightarrow F^-$), being a second-order process. When negative-ion conversion of F^0 projectiles passing above the LiF surface is taken into account, the decrease of the F^- formation in two-electron-capture events is compensated by F^- formation from fluorine atoms. In summary, we have two velocity domains for negative-ion formation. At projectile velocities smaller than 0.12 a.u., negative ions are formed via simultaneous two-electron-capture events, with two electrons captured from adjacent F^- sites at the surface. At high projectile velocities, negative ions are formed dominantly in two independent steps: $F^+ \rightarrow F^0$, then $F^0 \rightarrow F^-$.

In the low-velocity regime, the F^- formation from $F^+(^3P)$ projectiles is most efficient because of the best energy matching. At higher velocities, when the negative-ion formation from neutral projectiles is taken into account, the negative-ion fractions saturate. As it was already discussed for the negative-ion conversion of neutral projectiles, this saturation effect arises because our approach does not take into account the electron detachment for the negative ion flying above the crystal.[1,2]

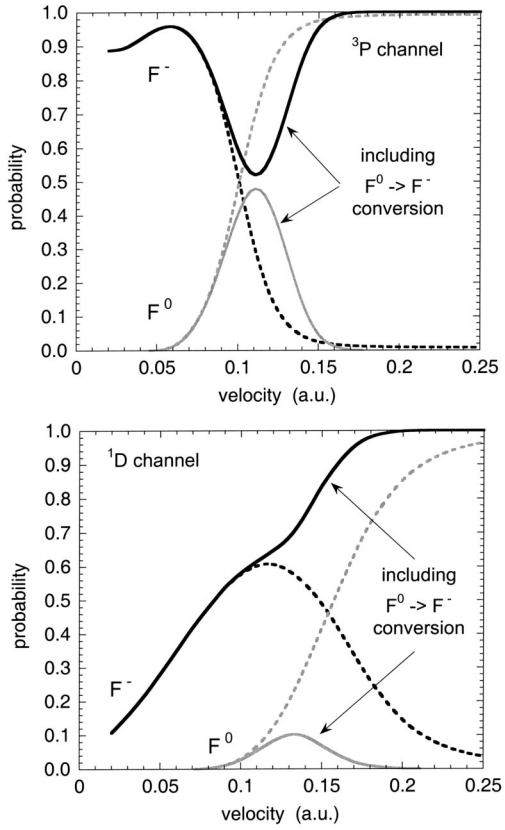

FIG. 8. (a) Calculated probabilities of negative-ion formation (black) and neutralization (gray) as functions of projectile velocity for $F^+(^3P)$ ions impinging on a LiF(001) surface close to the $\langle 100 \rangle$ direction at a grazing angle of incidence $\theta = 1°$ from the surface plane. Solid lines correspond to the results obtained when the negative-ion conversion of the F^0 atoms in binary collisions with F^- sites at the surface, $\Pi^-(Z)$ [see Eq. (10)], is taken into account. Dashed lines represent the results obtained when this negative-ion formation channel is neglected. (b) same as (a), but for $F^+(^1D)$ projectiles.

Results averaged over all possible states of the incident F^+ ions are compared with experimental data of Ref. 39 in Fig. 9. The calculated negative-ion formation probabilities saturate at the 0.933 level. This is because (i) the electron-loss process is not taken into account, and (ii) the $F^+(^1S)$ projectiles, constituting $\frac{1}{15}$ of the beam, do not undergo charge transfers within the considered velocity range. As follows from the calculated charge fractions, the sensitivity of the final results to a particular choice of the azimuthal direction is small. Therefore a comparison between the present theoretical results and experimental data taken at a random direction is meaningful. Our model calculations are able to explain the efficient negative-ion conversion of positive pro-

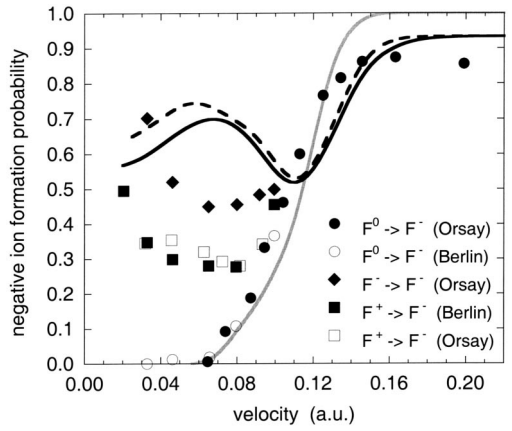

FIG. 9. Negative-ion formation probabilities in the scattered beam for grazing scattering ($\theta=1°$) of fluorine projectiles in different charge states from a LiF(001) surface. Experimental data of Ref. 39 (symbols) and present theoretical results (lines) are plotted as functions of the projectile velocity. All the experimental data are taken in random direction. Gray line represents the results for the negative-ion conversion of the neutral, F^0, projectiles as obtained in Refs. 24 and 45. Black solid and dashed lines represent the calculated negative-ion conversion probabilities for the F^+ projectiles scattered close to $\langle 100\rangle$ and $\langle 110\rangle$ directions, respectively.

jectiles at low velocities, i.e., below the threshold for the negative-ion conversion of neutral atoms.

While a qualitative agreement with the experiment is good, the present calculations overestimate negative-ion fractions. Indeed, the negative-ion fraction in the scattered beams is a result of the competition between electron capture and electron detachment. Although at low collision velocities the electron-loss probability is small because of the wide band gap of the LiF crystal, it cannot be neglected for a quantitative description of the negative-ion fractions.[2,9,25,39] This is evident from experimental data for F^- projectiles in Fig. 9. Since at low velocities the formation of F^- ions from neutral projectiles is not possible, finite negative-ion fractions in the scattered beam directly reflect the probability of negative-ion survival over the entire trajectory. The model outlined above provides the basis for a theoretical treatment of electron *capture*, incorporation of electron *loss* is left to future studies. Furthermore, the present calculations do not address the question of the population sharing between negative-ion and excited states at the surface when the newly formed F^- projectile recedes from the charge-transfer region.[9,10,17] Thus our calculations explain why at low velocities negative ions are formed much more efficiently from F^+ projectiles than from F^0 projectiles, but they are not intended to reproduce experimental data on a quantitative level. The quantitative comparison is, however, feasible on the basis of information derived from the energy-loss measurements.[39]

As discussed in Ref. 39, the negative ion formed in the binary-type collision process close to the surface gives rise to several final states of the projectile-LiF system. First, the negative ions are formed in the scattered beam ($F^+ \rightarrow F^- + LiF^{2+}$). In addition, the F^- ion can play a role of an efficient intermediate leading to the electron emission ($F^+ \rightarrow F^- + LiF^{2+} \rightarrow F^0 + e^- + LiF^{2+}$) or formation of the excited state at the surface termed trion ($F^+ \rightarrow F^- + LiF^{2+} \rightarrow F^0 + LiF^+ *$). All these channels were resolved in energy-loss measurements, in coincidence with electron emission. The key result of the data analysis is that, for 1 keV collision energy, almost 70% of the scattered products are connected with an initial F^- formation (see Table 1 of Ref. 39). Since negative-ion formation from neutral projectiles is not possible for slow collisions, the above result can directly be compared to a probability for F^- formation of 0.65 obtained theoretically (see Fig. 9). Thus, the inclusion of negative-ion destruction and trion formation in the present theoretical treatment may lead to a quantitative description of negative-ion conversion of F^+ projectiles.

V. CONCLUSIONS

We have reported on theoretical studies aimed to explain recent experimental results on the simultaneous two-electron capture in the negative-ion conversion of F^+ projectiles grazingly scattered from a LiF surface.[39] We show that the theoretical approach based on the model of energy-level confluence developed for the $F^0 \rightarrow F^-$ conversion[22–24] can be successfully applied to the double-electron capture. It is demonstrated that the direct $F^+ \rightarrow F^-$ conversion of the projectile with simultaneous capture of two electrons from adjacent F^- sites is a nearly resonant process. This is because the Coulomb interaction between the negative projectile and two holes in the final state of the charge-transfer reaction gives rise to the energy-level confluence. Since the F^+ ion has a $2p^4$ electronic shell structure, it may be produced in the ground $^3P^e$ and in the $^1D^e$ and $^1S^e$ excited metastable states. The model incorporates the presence of the latter states in the incident beam.

Our calculations are in good agreement with experimental data. In particular, we show that at low collision velocities (<0.1 a.u.), the F^- ions are produced as a result of the *simultaneous* capture of two electrons from neighboring halogen surface sites. The simultaneous two-electron-capture process by F^+ projectiles leads to large negative-ion fractions in the scattered beam well below the energy threshold for $F^0 \rightarrow F^-$ conversion. For higher projectile velocities, the negative ions are formed dominantly in two consecutive steps: $F^+ \rightarrow F^0$, then $F^0 \rightarrow F^-$. Since electron loss and the formation of excited states of the surface are not included in the present calculations, absolute negative-ion fractions are overestimated. On the other hand, the theoretical results are in close agreement with experimental probabilities summed over the three channels which are believed to have the F^- ion as a precursor: scattered F^- ion, scattered F^0 atom + emitted electron, scattered F^0 atom + surface excitation (trion). This gives confidence in the theoretical model and provides clear hints for its improvement.

ACKNOWLEDGMENT

This work was supported by the Deutsche Forschungsgemeinschaft (DFG, Grant No. Wi 1336).

APPENDIX A

This appendix describes the procedure used to construct the electronic basis states $\Phi_j(\{\boldsymbol{\rho}\};\mathbf{R})$ involved in the model described in Sec. II A [Eq. (5)] and the determination of the corresponding Hamiltonian matrix [Eq. (7)].

We follow ideas proposed earlier in gas-phase collision studies to build so-called (quasi-) diabatic states for charge-transfer processes which (except for Coriolis coupling) have the property of making the passage from Eq. (6) to Eq. (7) legitimate. The procedure resembles the projected valence bond method,[60,61] which emphasizes the charge-transfer arrangements by specifying the distribution of holes in the active molecule and the projectile, namely, $F^+ + {F_2}^{2-}$, $F^0 + {F_2}^-$, and $F^- + {F_2}^0$.

We start from a set of molecular orbitals for the ${F_2}^{2-}$ active molecule (in the absence of the projectile) and a set of atomic orbitals for the isolated projectile. Then, taking the ${F_2}^{2-}$-F^- closed-shell system as a reference, we generate all configuration state functions (CSF's) with singlet or triplet spin multiplicity that arises by distributing two holes between the six outer orbitals of the molecule and the three $2p$ orbitals of the projectile. At infinite separation of the active molecule and projectile, the Hamiltonian matrix in the singlet or triplet CSF basis is constructed and then diagonalized, thereby yielding the actual asymptotic states $\Phi_j(\{\boldsymbol{\rho}\};\mathbf{R}\rightarrow\infty)$ of the problem; the corresponding unitary transformation between the $\Phi_j(\{\boldsymbol{\rho}\};\mathbf{R}\rightarrow\infty)$ states and the CSF's is denoted by C_∞. For finite separations between the active molecule and the projectile, the orbitals are first orthonormalized by the Gram-Schmidt procedure in the following order: (inner shells of the molecule, inner shells of the projectile, valence shell of the molecule, valence shell of the projectile). Then, for each spin multiplicity, the Hamiltonian matrix is built in the CSF basis and then transformed to the $\Phi_j(\{\boldsymbol{\rho}\};\mathbf{R})$ basis using the C_∞ matrix. Thus the $\Phi_j(\{\boldsymbol{\rho}\};\mathbf{R}\rightarrow\infty)$ functions consist of constant linear combinations of CSF's built from orthonormalized asymptotic orbitals. Aside from a weak variation with $\mathbf{R}$ due to the orthogonalization of the orbitals, these states preserve at finite distances the dominant characters of the asymptotic charge-transfer states they correlate with.

All calculations have been carried out using the GAMESS quantum chemistry program.[53] The active diatomic molecule is embedded in a lattice of four layers made of alternating $+1$ and -1 point charges (Fig. 1). A total of 782 point charges has been used; this was found sufficient to accurately reproduce the Madelung potential of the LiF crystal. The set of molecular and atomic orbitals was obtained from Hartree-Fock-Roothaan SCF calculations on the F^--{embedded ${F_2}^{2-}$} closed-shell system at infinite atom-molecule separation. The calculations were performed using the SBKJC-31G effective core potential (see Ref. 62 for definition) and corresponding CGTO (contracted Gaussian-type orbital) expansion basis set.[62] The Hamiltonian matrices for 45 singlet states and 36 triplet states were obtained by distributing two holes in the relevant outer shells of the system as described above. The detailed analysis of the wave functions shows that the 12 upper states in the singlet case and the six upper states in the triplet case correspond to $F^- + {F_2}^0$ charge-transfer arrangements, with the two holes essentially localized on the same F^- site of the active molecule. These states are so high in energy relative to the initial $F^+ + {F_2}^{2-}$ channels that they have not been retained in the dynamics calculation.

It may rightfully be objected that the use of the single set of ${F_2}^{2-}$ and F^- orbitals introduces errors in the calculated energy levels of charge-transfer states involving the ${F_2}^-$, ${F_2}^0$, F^0, and F^+ species: The shell relaxation subsequent to the creation of one or two holes in the reference system is not taken into account. While this relaxation can, in principle, be taken into account by configuration-interaction (CI) calculations, the actual CI would require all possible rearrangements of 16 electrons among the considered nine outer orbitals of the reference system. The sizes of the C_∞ matrices in this latter case would have been larger than the considered ones by several orders of magnitude. This would make impossible the required systematic calculations. Therefore the errors in the energies (diagonal elements of the Hamiltonian matrices) have been corrected by adjusting the computed energy-level differences to experimental values known for infinite projectile surface separations.

It is also worth noting that the CGTO expansion basis does not include diffuse orbitals for the description of polarization or excited (low-lying Rydberg-like or excitonic) states. The main reason for that is essentially the same as that put forward above: the dramatic increase in size of the C_∞ matrices that would have arisen from excitations to the diffuse orbitals. The lack of the polarization effects should lead to a slight overestimation of the energy defects of the $F^+ + {F_2}^{2-} \rightarrow F^- + {F_2}^0$ charge-transfer reaction. Indeed, in the final state of the charge transfer, the F^- ion is polarized in the field of the two holes at the surface.

APPENDIX B

Here we discuss in greater detail the definition of the LiF ionization potential I_{LiF} (binding energy of valence-band electrons to F^- ions at the LiF surface). As follows from Eqs. (1), (2), and (3c), this is an important quantity controlling the energy balance of the charge-transfer reaction. This is especially the case for the $F^+ \rightarrow F^-$ charge-transfer reaction, where I_{LiF} enters with a factor 2. Since in our treatment

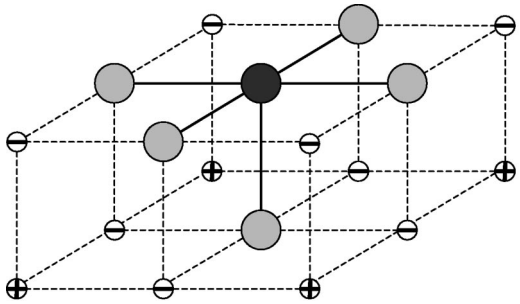

FIG. 10. The model $(Li_5F)^{4+}$ cluster imbedded in the point-charge lattice used to calculate the energy of the middle of the valence band of LiF. Dark circle, F^- ion; gray circles, Li^+ ions.

we neglect the hole migration in the crystal (finite valence-band width), I_{LiF} corresponds to the position of the VB center. The experimental information, available on the energies of the VB electrons in LiF reflects the situation where the hole left in the VB polarizes the crystal (infinite time limit). At the instant of charge transfer, the crystal polarization effects do not set in as explained in Sec. II A. Therefore we should seek a definition of I_{LiF} free of crystal polarization effects. For the simple point-charge model, I_{LiF} is given by the sum of the Madelung potential at an F^- site of the surface and the electron affinity of a free F^- ion. This yields $I_{\mathrm{LiF}}=15.45$ eV. This is the value used to plot the results in Fig. 2. This estimate does not take into account the difference between the Madelung potential at the center of the lattice site and that averaged over the $2p$ orbitals of the F^- ion. Moreover, the orthogonality constraint of the $F^-(2p)$ orbitals with respect to the $1s$ orbitals of the surrounding Li^+ ions may result in sizable corrections. We have performed an *ab initio* calculation of an $(FLi_5)^{4+}$ cluster embedded in the point-charge environment, as shown in Fig. 10. This results in the $I_{\mathrm{LiF}}=14.11$ eV value used in our charge-transfer calculations.

[1] H. Winter, Prog. Surf. Sci. **63**, 177 (2000).
[2] A. G. Borisov and V. A. Esaulov, J. Phys. C **12**, R177 (2000).
[3] R. Souda, T. Suzuki, H. Kawanowa, and E. Asari, J. Chem. Phys. **110**, 2226 (1999).
[4] P. Varga and U. Diebold, in *Low Energy Ion-Surface Interactions*, edited by J. W. Rabalais (Wiley, New York, 1994).
[5] V. Kempter, Comments At. Mol. Phys. **34**, 11 (1998).
[6] See the review articles in the book on *Low Energy Ion-Surface Interactions* (Ref. 4).
[7] M. Vana, F. Aumayr, and H. P. Winter, Europhys. Lett. **29**, 55 (1995).
[8] C. Auth, A. Mertens, H. Winter, and A. G. Borisov, Phys. Rev. Lett. **81**, 4831 (1998).
[9] P. Roncin, J. Villette, J. P. Atanas, and H. Khemliche, Phys. Rev. Lett. **83**, 864 (1999).
[10] A. Mertens *et al.*, Nucl. Instrum. Methods Phys. Res. B **182**, 23 (2001).
[11] G. Hayderer *et al.*, Phys. Rev. Lett. **83**, 3948 (1999).
[12] L. Wirtz *et al.*, Surf. Sci. **451**, 197 (2000).
[13] G. Hayderer *et al.*, Phys. Rev. Lett. **86**, 3530 (2001).
[14] T. Neidhart, F. Pichler, F. Aumaur, H. P. Winter, M. Schmid, and P. Varga, Phys. Rev. Lett. **74**, 5280 (1995).
[15] A. G. Borisov, A. Mertens, H. Winter, and A. K. Kazansky, Phys. Rev. Lett. **83**, 5378 (1999).
[16] J. Villette, A. G. Borisov, H. Khemliche, A. Momeni, and P. Roncin, Phys. Rev. Lett. **85**, 3137 (2000).
[17] H. Eder *et al.*, Phys. Rev. A **62**, 052901 (2000).
[18] H. Khemliche, J. Villette, A. G. Borisov, A. Momeni, and P. Roncin, Phys. Rev. Lett. **86**, 5699 (2001).
[19] P. A. Zeijlmans van Emmichoven *et al.*, Phys. Rev. B **59**, 10 950 (1999).
[20] R. Souda *et al.*, Surf. Sci. **324**, L349 (1995).
[21] R. Souda, Int. J. Mod. Phys. B **14**, 1139 (2000).
[22] C. Auth, A. G. Borisov, and H. Winter, Phys. Rev. Lett. **75**, 2292 (1995).
[23] C. Auth, A. Mertens, H. Winter, A. G. Borisov, and V. Sidis, Phys. Rev. A **57**, 351 (1998).
[24] A. G. Borisov and V. Sidis, Phys. Rev. B **56**, 10 628 (1997).
[25] S. Ustaze, R. Verucchi, S. Lacombe, L. Guillemot, and V. A. Esaulov, Phys. Rev. Lett. **79**, 3526 (1997).
[26] M. Richard-Viard *et al.*, Nucl. Instrum. Methods Phys. Res. B **164–165**, 575 (2000).
[27] K. Sekar *et al.*, Phys. Rev. B **63**, 045411 (2001).
[28] P. Stracke, F. Wiegershaus, St. Krischok, H. Müller, and V. Kempter, Nucl. Instrum. Methods Phys. Res. B **125**, 63 (1997).
[29] F. Meyer, Q. Yan, P. Zeijlmans van Emmichoven, I. G. Hughes, and G. Spierings, Nucl. Instrum. Methods Phys. Res. B **125**, 138 (1997).
[30] C. Auth, T. Hecht, T. Igel, and H. Winter, Phys. Rev. Lett. **74**, 5244 (1995).
[31] L. Hägg, C. O. Reinhold, and J. Burgdörfer, Phys. Rev. A **55**, 2097 (1997).
[32] L. Wirtz, C. Lemell, C. O. Reinhold, L. Hägg, and J. Burgdörfer, Nucl. Instrum. Methods Phys. Res. B **182**, 36 (2001).
[33] H. Khemliche, T. Schlathölter, R. Hoekstra, and R. Morgenstern, Phys. Rev. Lett. **81**, 1219 (1998).
[34] J. J. Ducrée, F. Casali, and U. Thumm, Phys. Rev. A **57**, 338 (1998).
[35] F. Wiegershaus, S. Krischok, D. Ochs, W. Maus-Friedrichs, and V. Kemter, Surf. Sci. **345**, 91 (1996).
[36] W. Fritsch and C. D. Lin, Phys. Rev. Lett. **61**, 690 (1988).
[37] L. F. Errea, B. Herrero, L. Mendez, and A. Riera, J. Phys. B **28**, 693 (1995).
[38] M. Barat and P. Roncin, J. Phys. B **25**, 2205 (1992).
[39] P. Roncin *et al.*, Phys. Rev. Lett. **89**, 043201 (2002).
[40] H. Tatewaki and E. Miyoshi, Surf. Sci. **327**, 129 (1995).
[41] M. Piacentini and J. Anderegg, Solid State Commun. **38**, 191 (1981).
[42] D. A. Lapiano-Smith, E. A. Eklund, F. J. Himpsel, and L. J. Terminello, Appl. Phys. Lett. **59**, 2174 (1991).
[43] F. J. Himpsel, L. J. Terminello, D. A. Lapiano-Smith, E. A. Eklund, and J. J. Barton, Phys. Rev. Lett. **68**, 3611 (1992).
[44] E. L. Shirley, Phys. Rev. B **58**, 9579 (1998).
[45] A. G. Borisov, J. P. Gauyacq, V. Sidis, and A. K. Kazansky, Phys. Rev. B **63**, 045407 (2001).
[46] J. Vogt and H. Weiss, Surf. Sci. **501**, 203 (2002).
[47] W. B. Fowler, Phys. Rev. **151**, 657 (1966).
[48] W. P. O'Brien, Jr. and J. P. Hernandez, Phys. Rev. B **9**, 3560 (1974).
[49] N. F. Mott and M. J. Littleton, Trans. Faraday Soc. **34**, 485 (1938).
[50] G. D. Mahan, Phys. Rev. B **21**, 4791 (1980).
[51] M. C. Torralba, C. M. Slutzky, E. A. Garcia, and E. C. Goldberg, Phys. Rev. B **63**, 195411 (2001).
[52] E. A. Garcia, P. G. Bolcatto, M. C. G. Passeggi, and E. C. Goldberg, Phys. Rev. B **59**, 13 370 (1999).
[53] GAMESS (Version 25 Mar 2000), Iowa State University; M. W. Schmidt, K. K. Baldridge, J. A. Boatz, S. T. Elbert, M. S. Gor-

don, J. J. Jensen, S. Koseki, N. Matsunaga, K. A. Nguyen, S. Su, T. L. Windus, M. Dupuis, J. A. Montgomery, J. Comput. Chem. **14**, 1347 (1993).
[54] C. Leforestier *et al.*, J. Comput. Phys. **94**, 59 (1991).
[55] D. S. Gemell, Rev. Mod. Phys. **46**, 129 (1974).
[56] P. M. Echenique and A. Howie, Ultramicroscopy **16**, 269 (1985).
[57] N. Arista, Phys. Rev. A **49**, 1885 (1994).
[58] E. D. Palik and W. R. Hunter, in *Handbook of Optical Constants of Solids* (Academic Press, New York, 1985).
[59] N. W. Ashcroft and N. D. Mermin, *Solid State Physics* (Saunders College, Philadelphia, 1976).
[60] C. Kubach and V. Sidis, Phys. Rev. A **14**, 152 (1976).
[61] V. Sidis, Adv. Chem. Phys. **92**, 73 (1992).
[62] SBKJC-31G splits (available Li-Rn); W. J. Stevens, H. Basch, and M. Krauss, J. Chem. Phys. **81**, 6026 (1984); W. J. Stevens, H. Basch, M. Krauss, and P. Jasien, Can. J. Chem. **70**, 612 (1992); T. R. Cundari and W. J. Stevens, J. Chem. Phys. **98**, 5555 (1993).